TOPICAL REVIEW — Physical research in liquid crystal

Thermo- and photo-driven soft actuators based on crosslinked liquid crystalline polymers*

Wei Gu(顾伟)[1], Jia Wei(韦嘉)[1], and Yanlei Yu(俞燕蕾)[1,2,†]

[1] *Department of Materials Science, Fudan University, Shanghai* 200433, *China*

[2] *State Key Laboratory of Molecular Engineering of Polymers, Fudan University, Shanghai* 200433, *China*

(Received 16 May 2016; published online 19 July 2016)

Crosslinked liquid crystalline polymers (CLCPs) are a type of promising material that possess both the order of liquid crystals and the properties of polymer networks. The anisotropic deformation of the CLCPs takes place when the mesogens experience order to disorder change in response to external stimuli; therefore, they can be utilized to fabricate smart actuators, which have potential applications in artificial muscles, micro-optomechanical systems, optics, and energy-harvesting fields. In this review the recent development of thermo- and photo-driven soft actuators based on the CLCPs are summarized.

Keywords: actuators, crosslinked liquid crystalline polymers, deformation

PACS: 61.41.+e, 82.50.Hp, 83.80.Xz, 61.30.Vx **DOI:** 10.1088/1674-1056/25/9/096103

1. Introduction

There have recently been many studies on the construction of actuators that function as energy transducers in electronics,[1,2] integrated optics,[3] microelectromechanical systems,[4] and medical and biomedical applications.[5,6] Generally, actuators are stimuli-responsive and can convert various forms of input energies into mechanical motions. In the literature, a variety of materials have been utilized to fabricate actuators, such as inorganic shape-memory alloys and piezoelectric materials.[7,8] However, the use of polymers to fabricate actuators would have many advantages because of their softness, low weight, high corrosion resistance, and easy fabrication features. One of the essential factors to select raw materials for actuators is the ability to be stimuli-responsive. Among all of the responsive polymers, crosslinked liquid crystalline polymers (CLCPs) appear to be especially attractive because of their superior characteristics combining the order of liquid crystals (LCs) and the excellent properties arising from the polymer networks. Because the mesogens tend to show alignment in CLCPs coupled with the elastic property of the polymer networks, the CLCPs can undergo large anisotropic deformations due to the alignment change induced by external stimuli, such as light, changes in temperature and electric field.[9–14] Highly depending on the alignment mode of the mesogens, several forms of macroscopic shape changes have been achieved, including contraction (expansion), bending (unbending), twisting, and other complex forms, which are of great use in the development of soft actuators. In this review, we focus on the recent development of thermo- or photo-driven soft actuators fabricated from the CLCPs and the existing challenges and opportunities in this field, since heat and light are easily attainable stimuli sources.

2. Thermo-driven CLCP actuators

When the temperature increases above the LC to the isotropic phase transition temperature, the LC order of the CLCP films decreases and the mesogens become disordered. Therefore, the CLCP films generally demonstrate contraction in the alignment direction of the mesogens. In contrast, when the temperature decreases below the phase transition temperature, the CLCP films experience an expansion process and revert to their original shape (Fig. 1). De Gennes *et al*. first put forward the concept of the CLCPs as artificial muscles by utilizing their large uniaxial contraction along the direction of the director axis.[15] He also theoretically predicted that the phase transition was possible to induce a large deformation of CLCPs.[16] Finkelmann prepared a CLCP film with polysiloxane main chain and LC side chain, which showed a contraction of 26% when heated to the isotropic state due to the change in molecular alignment.[17] Furthermore, they synthesized a new type of CLCP consisting nematic LC main chain and side chain. The polymer could experience an elongation of 400% in the nematic state compared to the length in the isotropic state.[18] This superior property improved the ability of CLCPs to function as artificial muscles. Since then, a number of studies have been done on artificial muscle-like CLCPs.[19–21]

*Project supported by the National Natural Science Foundation of China (Grant Nos. 21134003, 21273048, 51225304, and 51203023) and Shanghai Outstanding Academic Leader Program, China (Grant No. 15XD1500600).

†Corresponding author. E-mail: ylyu@fudan.edu.cn

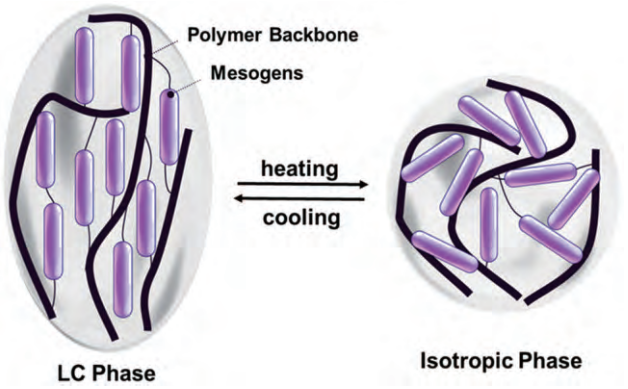

Fig. 1. (color online) A schematic illustration of the thermal induced anisotropic contraction and expansion of the CLCPs.

The alignment of mesogens within the CLCP films plays an important role in determining how the films deform. The CLCP films with a splay molecular alignment prepared by Broer *et al.* displayed a well-controlled deformation as a function of temperature, while the films with a twist structure showed a complex macroscopic deformation due to the formation of saddle-like geometries.[22] Urayama *et al.* found that the twist CLCP films could form helicoids or spiral ribbons, which depended on the competition between the in-plane elastic energy cost and the bending energy cost.[23] As Fig. 2 shows, the CLCP films with a small width-to-thickness ratio were easier to be stretched than to be bent and thus form helicoids; while, in contrast, those with a large width-to-thickness ratio were more likely to be bent than to be stretched and thus form spiral ribbons. In both cases, the ribbons experienced handedness reversal upon heating. Recently, White *et al.* developed an optical patterning system in which the polarization of an irradiating 445-nm laser was dynamically controlled over an area as small as 0.01 mm^2.[24] Therefore, the director of the LC molecules was programmable within local volume elements (voxels) as small as 0.0005 mm^3. A voxelated CLCP film containing nine defects in a square array is shown in Fig. 3(a) and the network structure is shown in Fig. 3(d). Each +1 defect is a point around which the director varies azimuthally by 360°. Macroscopic azimuthal contraction (along the director) and radial expansion around each defect center led to the emergence of cones (Fig. 3(b)). Figure 3(c) shows a characteristic photograph of an actuator with an array of four defects lifting a load 147 times heavier than itself and generating a stroke of ∼ 3000%. This giant stroke arose from the amplification of the intrinsic shape change (∼ 55% contraction) through a combination of localized stretching and delocalized bending. These materials with programmable mechanical response offered the possibility to produce monolithic multifunctional devices or function as reconfigurable substrates for flexible devices in medicine, aerospace, and consumer goods.

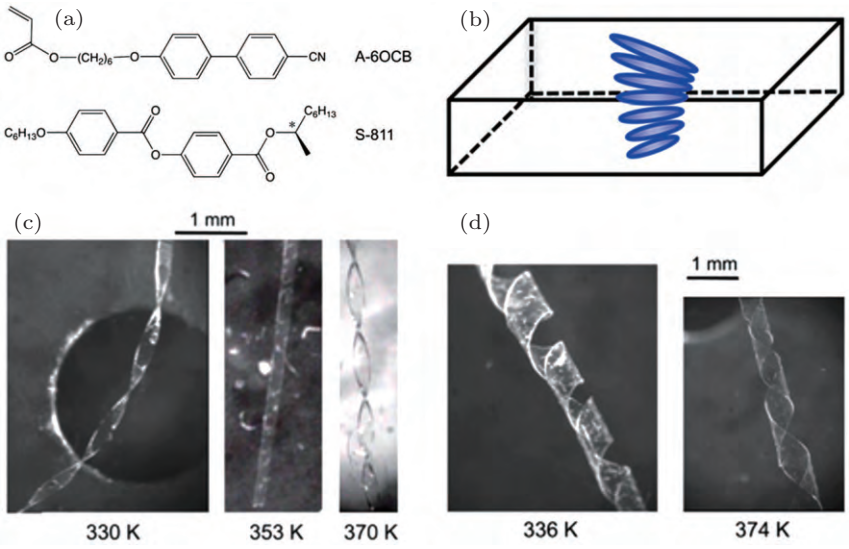

Fig. 2. (color online) (a) Monomer A-6OCB and chial dopant S-811 used in the study. (b) Schematics of the director orientation of twist nematic CLCP ribbons. Handedness reversal of (c) helicoids and (d) spiral ribbons formed by the narrow and the wide CLCP films, respectively. Reprinted with permission from Ref. [23].

Microelectromechanical systems (MEMs) have recently attracted strong interest in academic and industrial areas, and are fabricated by integrated mechanical elements, sensors, actuators, and electronics on a silicon substrate.[25] This emerging technology has caused a strong demand for micro- and nanometer-scaled actuators. Zentel *et al.* presented the use of a microfluidic setup to fabricate monodomainic, monodisperse, and micrometer-sized CLCP beads, the shape of which reversibly changed to a cigar-like conformation with the length increase of one axis by up to 70% (Fig. 4(b)).[26,27] This provided a new way to prepare micrometer sized actuators. After that, they successful realized the continuous fabrication of one-piece micropumps, LC core–shell polymer particles, through a microfluidic double-emulsion process, which re-

quired no elaborate micromachining techniques (Fig. 4(a)).[28] When the temperature increased to the isotropic phase at 130 °C, the CLCP shell experienced a deformation resulting from the phase transition and generated a force. The liquid glycerol within the core was, therefore, pushed into the capillary. Once the temperature cooled back to the nematic phase at 90 °C, the particle reverted to its former shape and the glycerol sank to its original level (Fig. 4(c)). They also utilized this setup to prepare the main-chain CLCP filament that was crosslinked in a continuous way by ultraviolet (UV) irradiation. The fiber actuator could lift a weight more than a thousand fold of its own weight.[29]

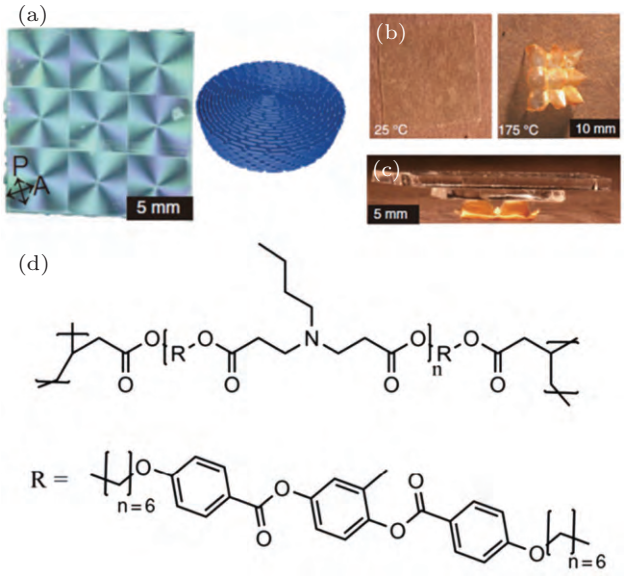

Fig. 3. (color online) (a) Representative photograph of CLCP film with nine +1 topological defects between crossed polarizers. The director orientation varies azimuthally around the defect. (b) Nine cones arise from the CLCP film upon heating. (c) Actuation with four +1 topological defects occurs in the presence of loads tens of times larger than the actuator weight. (d) Schematic of chemical structure of the main-chain CLCP that can be surface-aligned. Reprinted with permission from Ref. [24].

Except for the microfluid technique, there are some other ways of fabricating microactuators. By means of a soft lithography technique, researchers succeeded in producing micron-sized responsive CLCP pillars (Fig. (5a)).[20,21,30] When heated above the nematic to isotropic transition temperature, the individual pillars underwent ultralarge and reversible contractions of around 300–400% (Fig. 5(d)).[30] What is more, the reversible contraction along the axis of the pillar resulted in a roughness change of the microstructured surface. The water contact angle (CA) of the structured surface could be switched between 110° and 86° when the temperature varied between 35 °C and 80 °C (Fig. 5(f)).[31] In addition, nanowires were successfully prepared from a CLCP material with porous anodized aluminum oxide as templates. The high degree of order in the nanowires led to a strong change of their lengths during the phase transition.[32]

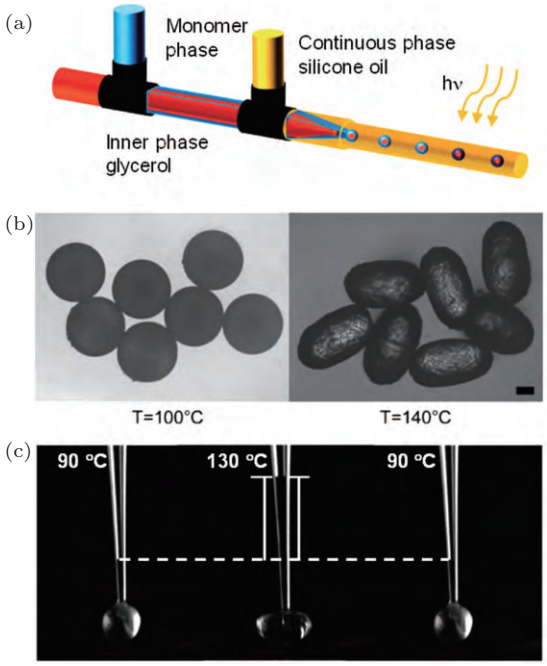

Fig. 4. (color online) (a) The microfluidic set-up used to prepare the CLCP shell particles filled with a glycerol core. Reprinted with permission from Ref. [28]. (b) Several CLCP particles fabricated by microfluidic setup in the LC phase and in the isotropic phase. Reprinted with permission from Ref. [26]. (c) Core-shell CLCP particles work as micropumps. Reprinted with permission from Ref. [28].

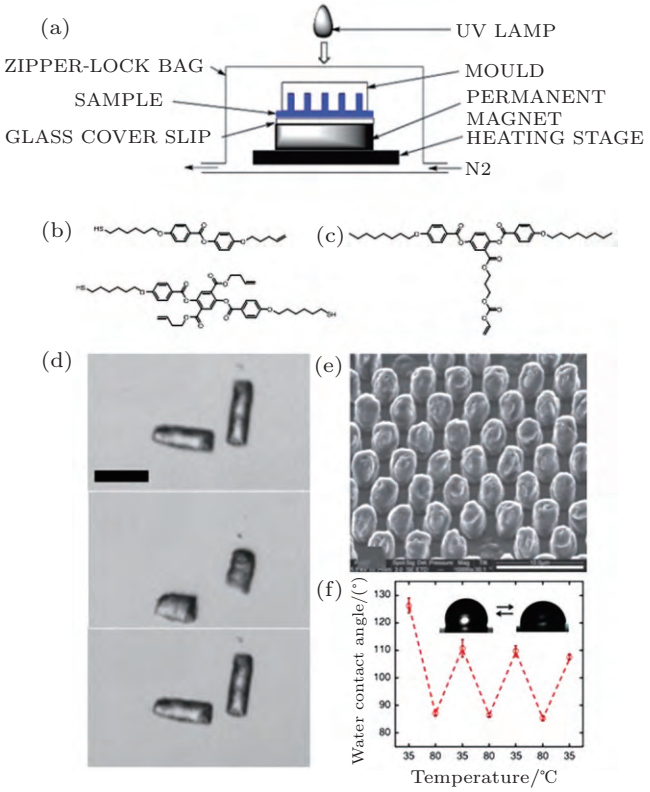

Fig. 5. (color online) (a) Experimental setup allows the preparation of the responsive pillars. Reprinted with permission from Ref. [21]. (b) The monomer and the crosslinker used to fabricate the main chain CLCP pillars in panel (d). (c) The LC monomer used to prepare the responsive microstructured CLCP surface in panel (e). (d) Contraction of isolated nematic main-chain CLCP pillars upon heating. Reprinted with permission from Ref. [30]. (e) Microstructured CLCP surface. Scale bar: 10 μm. (f) Cyclic measurements of the water CA for the microstructured CLCP surface. Insets are representative profiles of a water droplet on the surfaces. Reprinted with permission from Ref. [31].

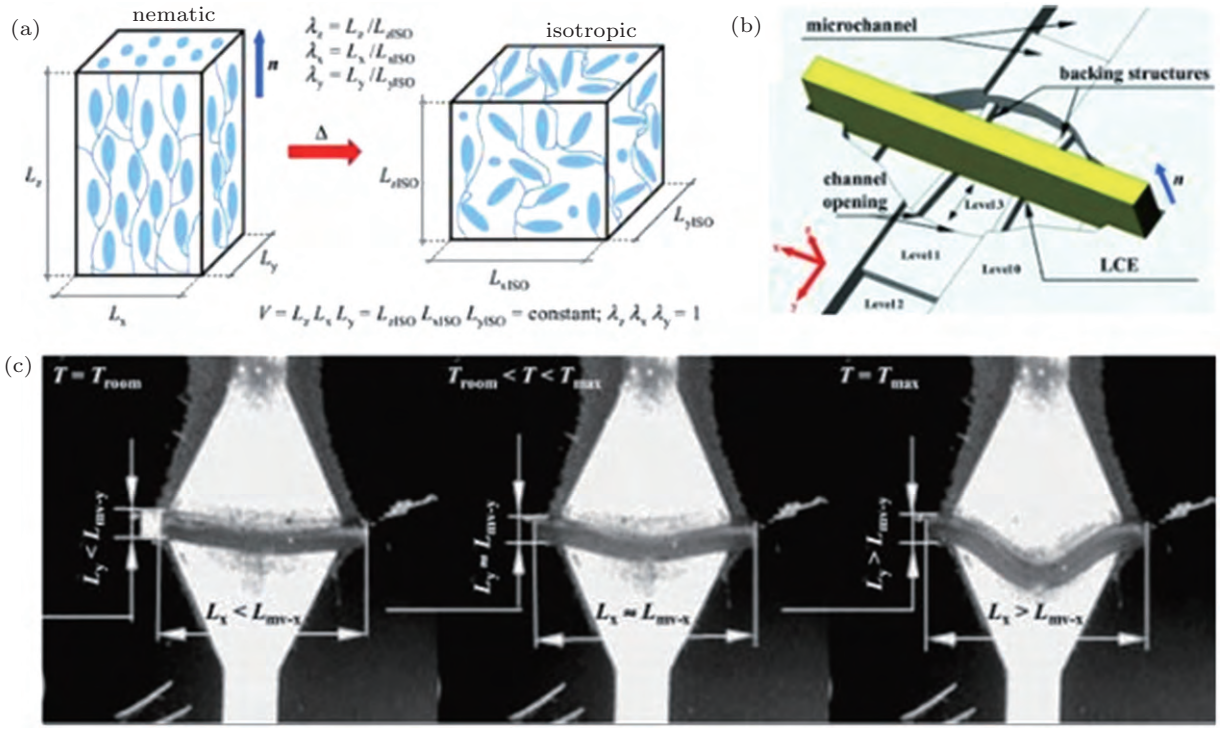

Fig. 6. (color online) (a) Nematic and isotropic states of a nematic side-chain CLCP. (b) Solid model of a half of the CLCP microvalve. (c) Snapshot photos during the actuation of the CLCP microvalve before the assembly of the microchip. Reprinted with permission from Ref. [34].

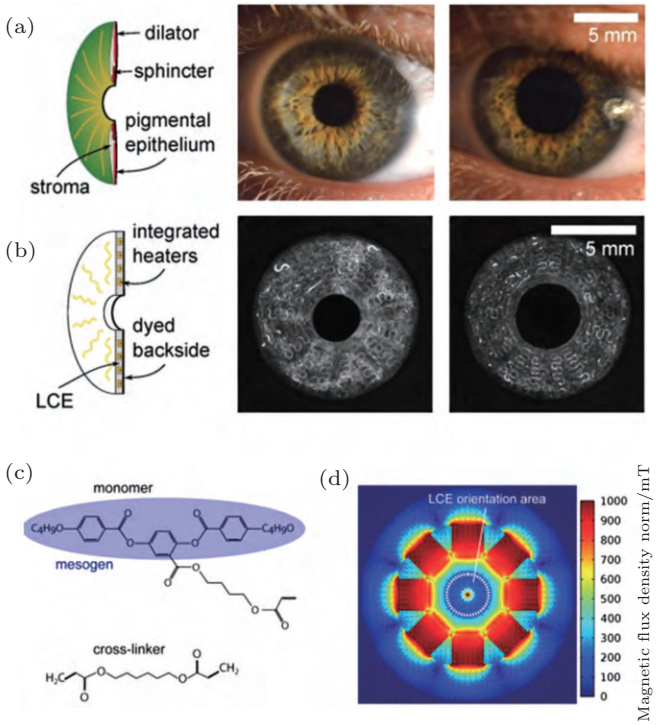

Fig. 7. (color online) (a) Schematic representation of the human iris exhibiting the tangentially contraction of sphincter muscle and the radially contraction of dilator muscle. (b) The CLCP iris with integrated polyimide-based platinum heaters contracts and expands in a way similar to that of the human iris. (c) The monomer and crosslinker used in the experiments. (d) Simulation of the magnetic field of the designed magnet with a continuous radial field in the orientation area that lies above the minimal magnetic field strength. Reprinted with permission from Ref. [35].

The studies of CLCP actuators in micro- and nano-scale open a door to their applications in microsystems, but it is more attractive to integrate CLCPs with other materials for the development of microsystem technology.[33] Sánchez-Ferrer *et al*. successfully integrated an oriented nematic side-chain CLCP into a silicon-based microstructured device for the application as a microvalve for microfluidics (Fig. 6).[34] They took advantages of both the expansion perpendicular to the director and the shrinkage parallel to the director to control the microvalve. The volumetric flow rate could be stopped just in one direction.

Schuhladen *et al*. showed the application of the CLCPs in optics for the first time.[35] They implemented a circularly symmetric actuation of radially oriented CLCPs to realize a tunable aperture, which mimicked the construction of the human iris. The orientation of the CLCPs was achieved by use of optimized, custom-designed radially oriented magnetic fields. Moreover, stretchable polyimide-based platinum heaters were embedded into the CLCPs to obtain fast and uniform heating. The resultant iris-like aperture was tunable by electrically actuated thermal means, which might have a significant potential in miniaturized photographic optics (Fig. 7).

3. CLCP soft actuators driven by remote heating

The development of thermo-driven actuators has been restricted in practical applications because of the difficulty to implement contactless and precise control. To this end,

many efforts have been made through absorptive heating with either optical or magnetic stimuli.[36,37] Therefore, carbon nanoparticles,[38] magnetic nanoparticals or nanorods,[39–41] carbon nanotubes,[42–46] and gold nanoparticles[47] were added to the CLCPs, which provides the possibility to cause thermal phase changes locally in their environment, since the absorption of photons by carbon nanotubes or gold nanoparticles is radiated as heat and heat transfer triggers thermomechanical effects in the CLCPs. The magnetic nanoparticles are known to transfer energy from electromagnetic irradiation into heat owing to relaxation processes.

Schenning *et al*. used the photoalignment technique to align polymerizable LCs and prepare freestanding CLCP films with complex alignment.[48] The setup for the preparation of patterned alignment cells is shown in Fig. 8(a). CLCP films with azimuthal and radial alignments were successfully prepared using the LC mixture comprising an IR-absorbing dye (Lumogen 788 IR) (Fig. 8(b)). The films deformed into conical and anti-cone shapes when heated by absorbing IR light (Figs. 8(c) and 8(d)). Regarding the azimuthal alignment pattern, the LC order decreased upon the increase of temperature, which led to compression along the azimuthal direction and expansion along the radial direction. Consequently, a conical shape was observed, as shown in Fig. 8(c). The opposite deformations took place concerning a radial alignment pattern, resulting in an anti-cone shape (Fig. 8(d)).

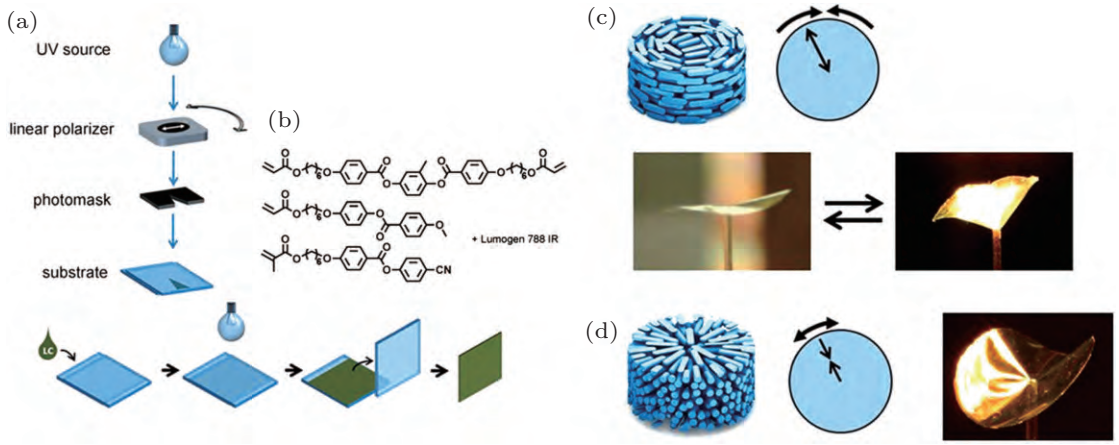

Fig. 8. (color online) (a) Setup for the fabrication of patterned alignment cells and procedure for making a patterned polymer LC. (b) LC mixture used for preparing the CLCP actuators. Actuation behavior of (c) an azimuthal CLCP film and (d) a radial CLCP film upon heating with an IR light. The arrows indicate the direction of deformation. Reprinted with permission from Ref. [48].

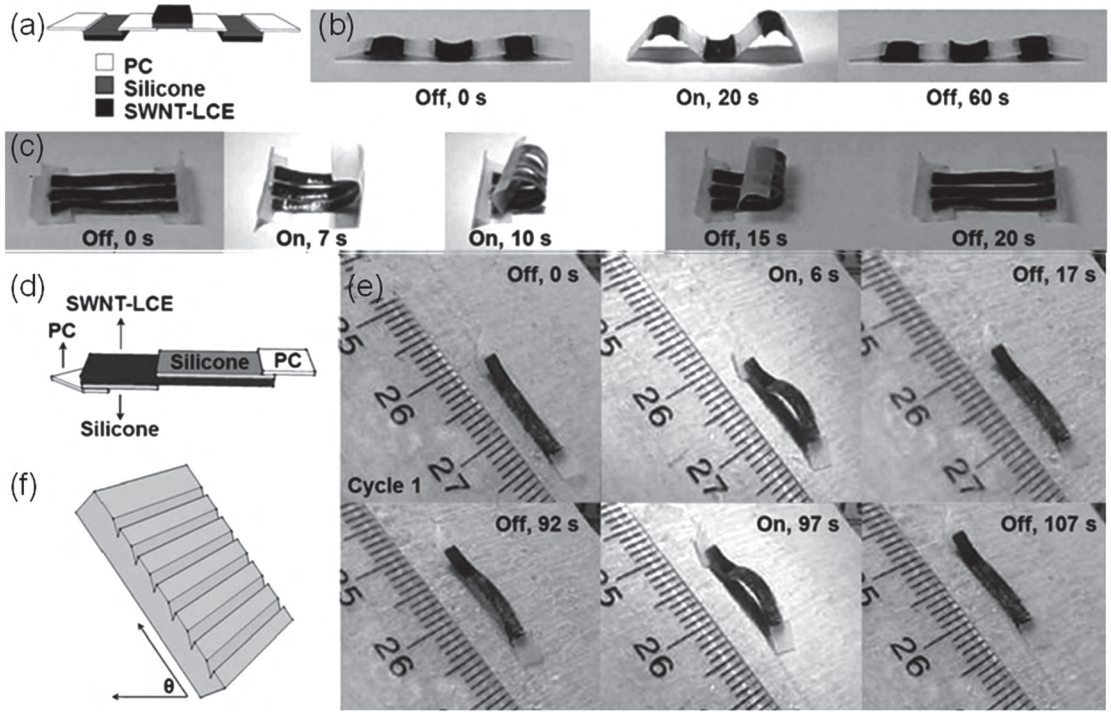

Fig. 9. (a) Schematic diagram of an origami structure. (b) Reversible folding and unfolding of the origami structure exposed to continuous-wave (CW) NIR light. (c) Reversible closing and opening motion of a Venus flytrap-inspired gripper exposed to CW NIR light. (d) Schematic diagram of an inchworm walker device. (e) Schematic diagram of a ratcheted wood substrate. (f) The inchworm walker crawling up the wood substrate at a 50° incline exposed to on and off cycles of CW NIR light. Reprinted with permission from Ref. [49].

Similarily, Chen *et al*. prepared IR light-driven bilayer hinges comprising one active CLCP composite layer with IR-active fillers and one passive silicone layer. The IR-active fillers consisted of single-walled carbon nanotubes (SWCNTs) and near IR dyes which generated heat by absorption of light.[49] The bilayer hinges could exhibit fast, reversible bending with a large strain due to the nematic–isotropic phase transition of the bulk CLCP. The bilayer films were fabricated into an active origami structure and an inchworm walker when assembled with polycarbonate (PC) films. The foldable origami structure inspired by a Venus flytrap opened and closed repeatedly when exposed to IR light (Fig. 9(c)). The inchworm walker could further crawl up the wood substrate at a 50° incline upon IR light irradiation cycles (Fig. 9(e)). What is more, the gripper composed of PC films and bilayer hinges was able to pick up and place various objects.

As mentioned above, the CLCP materials are capable of transferring optical or thermal energy into mechanical energy. Hence, they have promising applications in artificial muscles and MEMs. From an energy point of view, it is also fascinating to harvest solar energy and transfer it into electricity. Jiang *et al.* demonstrated artificial heliotropism for solar cells, utilizing polyurethane fiber-network/SWCNT/CLCP actuators that could be directly driven by the sunlight. Figure 10(a) shows the heliotropic behavior of the actuators. The solar cells are installed on a platform that is connected to the actuators. SWNTs absorb and transform the incoming sunlight into thermal energy, so that the actuators are in a contracted state toward the direction of the incident light at any time instant. While other actuators not irradiationd by the sunlight are in their original state. As a result, the platform holding the solar cells is driven by the contracted actuators, and self-adaptively tilts towards the sunlight.[50] The artificial heliotropism of the devices successfully worked with 60° of range in altitude angle and 180° of range in azimuth angle and the resultant output photocurrent of the solar cells increased significantly.

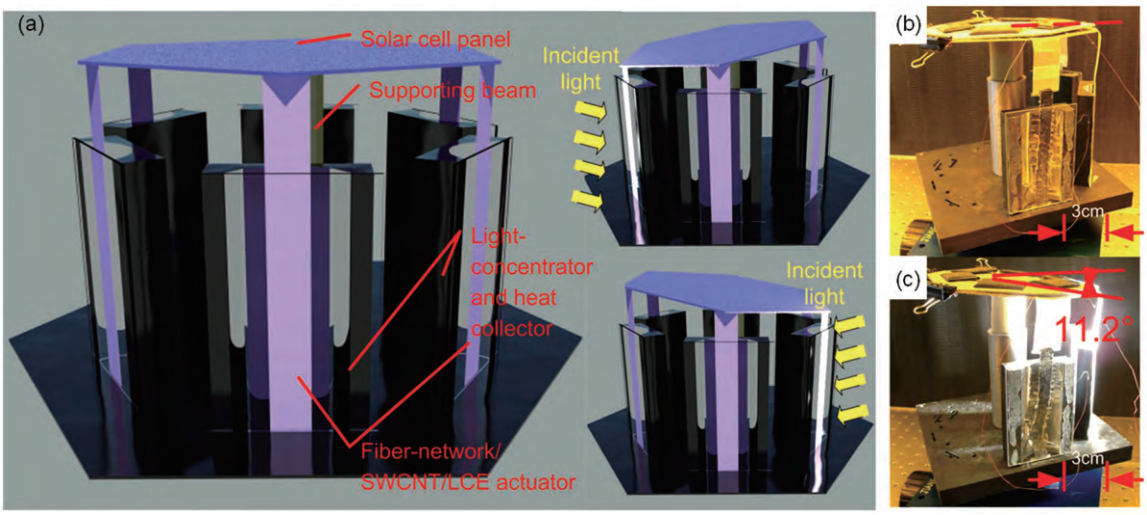

Fig. 10. (color online) (a) Three-dimensional (3D) schematic representation of the heliotropic behavior. (b), (c) Photographs showing the contraction of the actuator facing the sun, and the resultant tilt movement of the solar cell. Light source intensity: 100 mW/cm^2. Reprinted with permission from Ref. [50].

4. Light-driven CLCP soft actuators

If a few LC molecules change their order, the other LC molecules also change their alignment due to the cooperative effect of the LC molecules, indicating that only a small amount of energy is required to vary the alignment of the whole system. When a small quantity of photo-chromic molecules such as azobenzenes, stilbenes, and spiro-pyran derivatives are incorporated into LCs, the mixture can go through an LC-isotropic phase transition isothermally on exposure to light as a result of photochemical reaction of the photo-chromic molecules.[13,37,51–53] Azobenzenes are one of the typical photo-chromic molecules which have two isomerization states.[54–56] The thermally stable trans form of the azobenzene has a rodlike shape, which stabilizes the phase structure of the LC phase, while the meta-stable cis form is bent and tends to destabilize the phase structure (Fig. 11). This trans-cis photoisomerization gives rise to variations in physicochemical properties of the materials, such as polarity and molecular length.[13,57] The introduction of azobenzenes to the CLCPs results in fascinating photoresponsive systems of which the deformation can be triggered by light. In 2001, Finkelmann *et al.* succeeded in inducing a contraction ratio of 20% in the CLCPs with polysiloxane main chains and azobenzene crosslinkers by utilizing the trans-cis isomerization of azobenzene chromophores triggered by UV light.[58] After irradiation was stopped, the CLCPs restored to the original state owing to the thermal relaxation process of the azobenzene mesogens.

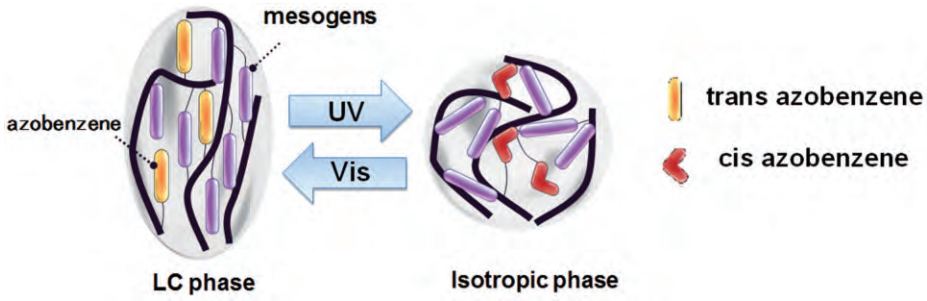

Fig. 11. (color online) Schematic diagram demonstrating photoisomerization of the azobenzene chromophores and photochemical phase transition of the azobenzene-containing CLCPs.

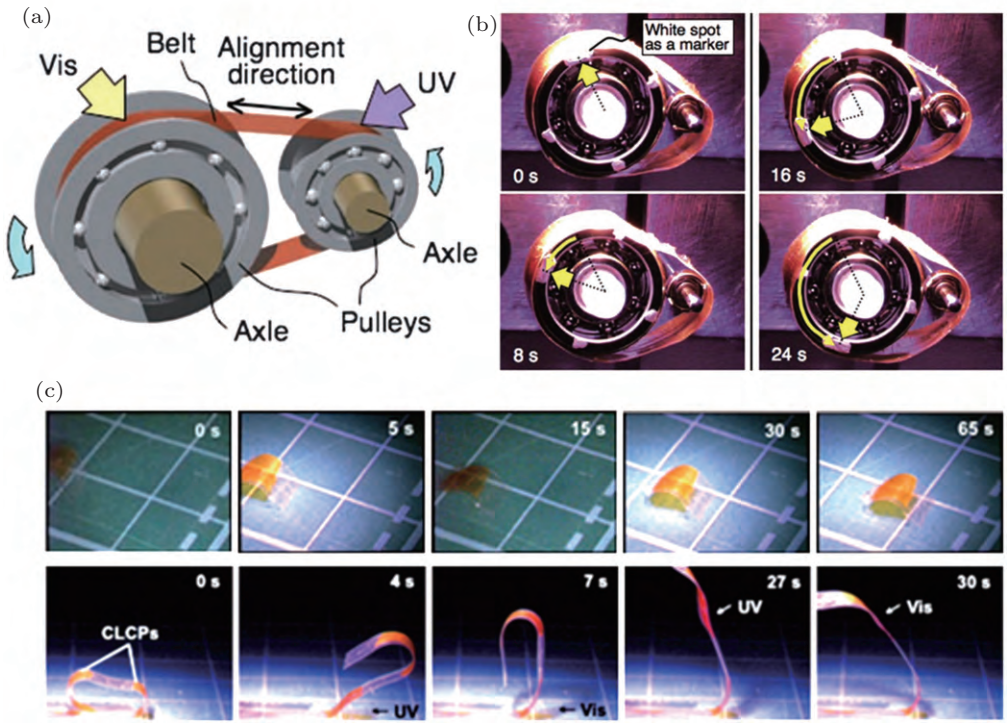

Fig. 12. (color online) (a) Schematic diagram of a photo-driven plastic motor system. Reprinted with permission from Ref. [61]. (b) Series of pictures exhibiting the rotation of the photo-driven plastic motor induced by simultaneous UV and visible light irradiation. Size of the belt: 36 mm × 5.5 mm. Reprinted with permission from Ref. [61]. (c) The photoinduced inchworm walk and the flexible robotic arm motion of the CLCP laminated film by alternate irradiation with UV and visible light. Sizes of the inchworm and the robotic arm are 11 mm × 5 mm and 34 mm × 4 mm, respectively. Reprinted with permission from Ref. [62].

Due to the large molar extinction coefficient of azobenzene moieties at around 360 nm, photons are absorbed only in the surface region of the CLCP films with a depth of several tens of micrometers. Therefore, the trans-cis photoisomerization only happens in the surface area, which leads to the bending motion of the CLCP films towards the light source.[59] Ikeda *et al.* succeeded in preparing a polydomain CLCP film consisting of many micron-sized domains that could be bent along a precisely controlled direction by irradiation with linearly polarized light.[60] Although macroscopically the direction of alignment was random, the azobenzene LC moieties aligned in one direction in each microdomain of the CLCP film. Upon irradiation with linearly polarized light, the azobenzene moieties aligned along the light polarization direction underwent trans-cis isomerization, which caused the bending movement of the CLCP film.

From the viewpoint of actuators, Ikeda *et al.* have successfully developed the first light-driven plastic motor with CLCP and flexible polyethylene (PE) laminated films.[61] The plastic motor was assembled with a belt fabricated by connecting both ends of the CLCP laminated film and a homemade pulley system as illustrated in Fig. 12(a). When irradiated with UV light from top right and visible light from top left simultaneously, the belt rotated and drove the two pulleys in a counterclockwise direction at room temperature. Upon UV light irradiation, a local contraction force was generated along the alignment direction of the azobenzene mesogens, which was parallel to the long axis of the belt. This contraction force led the right pulley to rotate in the counterclockwise direction. At the same time, a local expansion forced produced by visible light irradiation caused a counterclockwise rotation of the left pulley. Therefore, these simultaneous contraction and ex-

pansion forces generated at the different parts along the long axis of the belt resulted in the rotation of the pulleys and the belt with the same direction. The motor system rotated continuously because new parts were brought to the exposure of UV and visible light.

The composition of a CLCP and a flexible PE film also provided a variety of simple devices that walked in one direction like an 'inchworm' or moved like a 'robotic arm' whose movement was induced by light (Fig. 12(c)).[62] The inchworm had asymmetric end shapes. Upon alternate irradiation with UV and visible light, the sharp and flat edges of the inchworm acted as the stationary point, respectively. As a result, the inchworm walked in only one direction.

For applications of light-driven CLCP soft actuators in real applications, visible light is more advantageous because it is less harmful and abundant in sunlight. Our group prepared the CLCP films with a longer conjugated azotolane structure which transferred solar energy directly into mechanical energy.[63,64] Furthermore, we prepared a visible-light-driven microrobot by the combination of the CLCP and PE films, which was manipulated to pick, lift, move, and place milligram-scale objects by irradiating different parts (Fig. 13).[65] Upon visible light irradiation on the hand and wrist in succession, the hand opened and was made to close to the object. Due to the closing motion, the hand grasped the object after the light was off. The arm successfully lifted and moved the object to the container with irradiation of visible light. Finally, the hand placed the object into the container when irradiated with light on its back.

We also made use of the bending of the CLCP films to activate a pump membrane[66] and serve as a valve membrane.[67] The CLCP film actuator was initially pressed on the valve seat surface because a preload between inlet and outlet was applied on it. The valve was closed because the fluid in the inlet channel could not access the outlet channel. Upon UV light irradiation on the film from the bottom of the experimental setup, the valve was opened, as illustrated in Fig. 14(b), because the torque produced in the film was able to overcome the preload applied on it. Upon irradiation with UV light of 50 mW/cm^2, it took nearly 5 s to open the microvalve when the preload was 490 Pa, and 18 s when the preload was 3430 Pa (Fig. 14(d)). This photo-driven microvalve had small volume with low weight. In addition, using light as driving power made them applicable in battery-free devices.

Nature provides valuable inspirations for many research fields. Inspired by plant-like helical deformations, such as tendril coiling, spasmoneme springs, and seed pod opening, Fletcher *et al.* designed, synthesized, and studied the versatile actuation modes of photoresponsive CLCP springs (Fig. 15).[68] A few chiral molecule S-811 was doped into the mixture to induce a left-handed twist. The resultant orientation of the LC director changed smoothly by 90° from bottom to top surface. As Fig. 15(a) shows, the direction in which the ribbon was cut determined the pitch, the handedness of the helical shapes, and the photoresponsive behaviors. Under light irradiation, left-handed spiral ribbons showed a decrease in macroscopic pitch, and the relevant right handed ribbons increased their macroscopic pitch. Interestingly, inversion of the helical sense from right-handed to left-handed was also

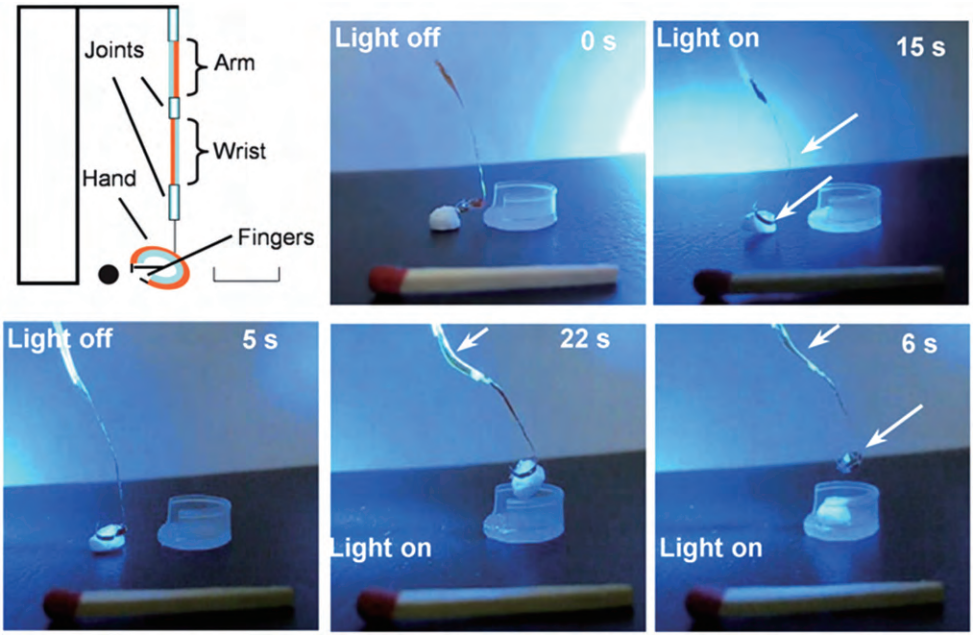

Fig. 13. (color online) Schematic illustration and pictures demonstrating the microrobot picking, lifting, moving, and placing the object to a nearby container by turning on and off the light (470 nm, 30 mW/cm^2). Thickness of PE and CLCP films: 12 mm. Object weight: 10 mg. Reprinted with permission from Ref. [65].

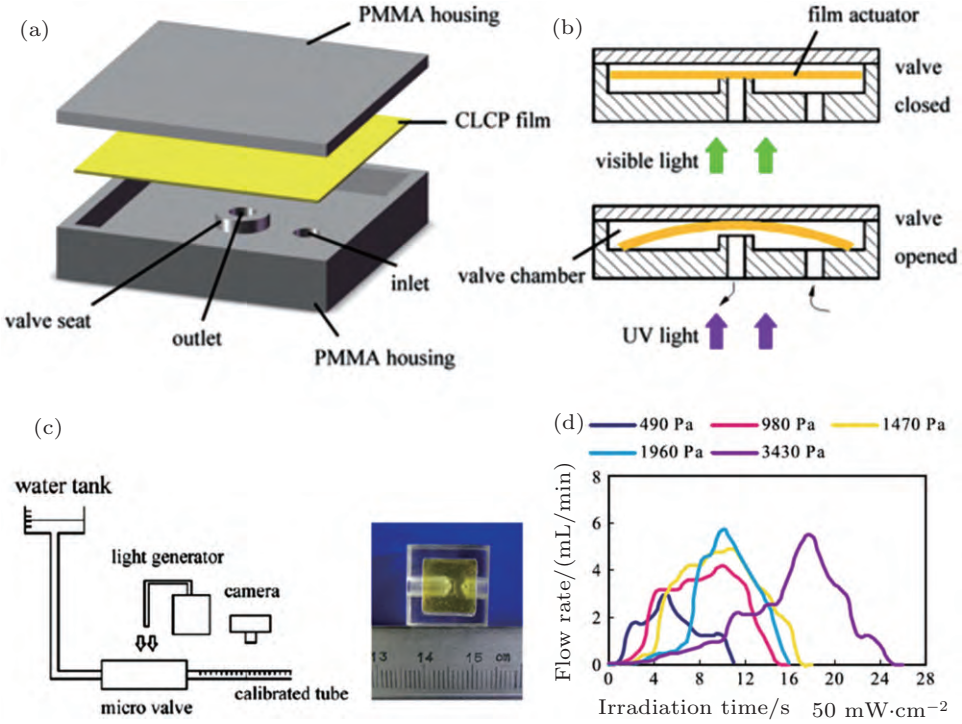

Fig. 14. (color online) (a) The schematic diagram of the light-activated microvalve model. (b) The cross section structure and the working principle of the photo-driven microvalve. (c) The experimental setup used to test the microvalve and the photograph of the microvalve. (d) Flow rate testing result of the microvalve (UV intensity: 50 mW/cm^2). Reprinted with permission from Ref. [67].

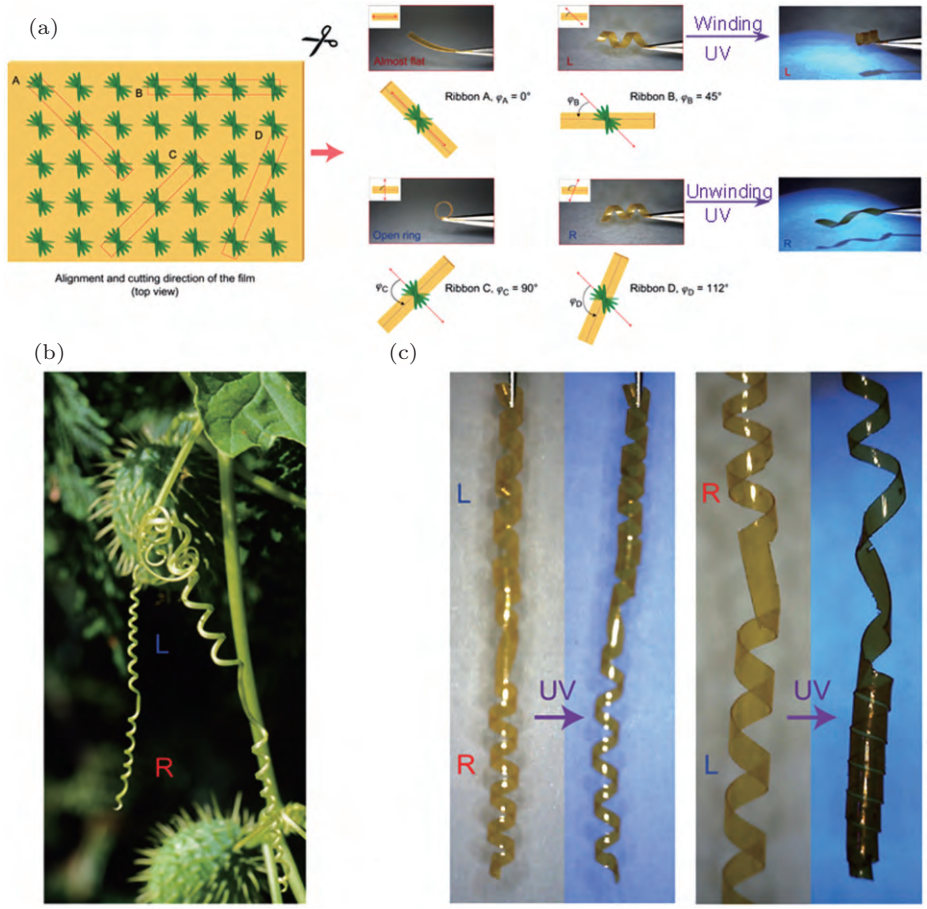

Fig. 15. (color online) (a) The CLCP ribbons exhibit various shapes depending on the cutting direction (Ribbon A: flat; Ribbon B: left-handed; Ribbon C: open ring; Ribbon D: right-handed). Ribbon B and Ribbon D show winding and unwinding under UV light irradiation for two minutes. (b) A coiled tendril of the wild cucumber plant. (c) A cucumber tendril-like polymer spring with two oppositely handed helices. The right-handed helix unwinds and the left-handed helix winds upon UV light irradiation. Reprinted with permission from Ref. [68].

possible to be observed. As a result, these springs displayed complex motion, including winding, unwinding, and helix inversion, which depended on the handedness of the director twist and the cutting direction. Depending on the orientation of the molecules, the ribbons always deformed to adapt to the preferred distortion along the main axis of the ribbon. The molecular orientation was, in turn, decided by the cutting direction. The mixed-helicity springs comprising two opposite handed helices displayed unwinding and winding motion simultaneously under UV irradiation, which successfully mimicked the movements of plant tendrils (Figs. 15(b) and 15(c)).

Van Oosten *et al.* presented a new method for developing cilia-like microactuators using an inkjet printing process followed by photopolymerization.[69] They used two dyes changing the composition of the actuator in the plane, the chemical structures of the two dyes DR1A and A3MA are shown in Fig. 16(a). The splayed molecular alignment in the film made the direction of the response is kept the same regardless of the direction of the incident light and generated stronger bending (Fig. 16(b)). Therefore, the position of the actuator could be brought into four positions by selecting the color composition of the light. When irradiated with only UV light, the yellow A3MA dyed part of the actuator bent. When irradiated with both UV and visible light, the total flap bent. Finally, if only visible light was used, only the red DR1A dyed part of the flap bent (Figs. 16(c) and 16(d)). Switching between these four positions produced a cilia-like motion, which was well controlled simply by changing the color of the light. This design provides the possibility to work in wet environments and is superior to the actuators driven by electrical fields. Moreover, the inject printing processing allows fabrication of large-area and roll-to-roll active all-polymer devices and opens up possibilities for rapid prototyping of low-cost micromechanical systems.

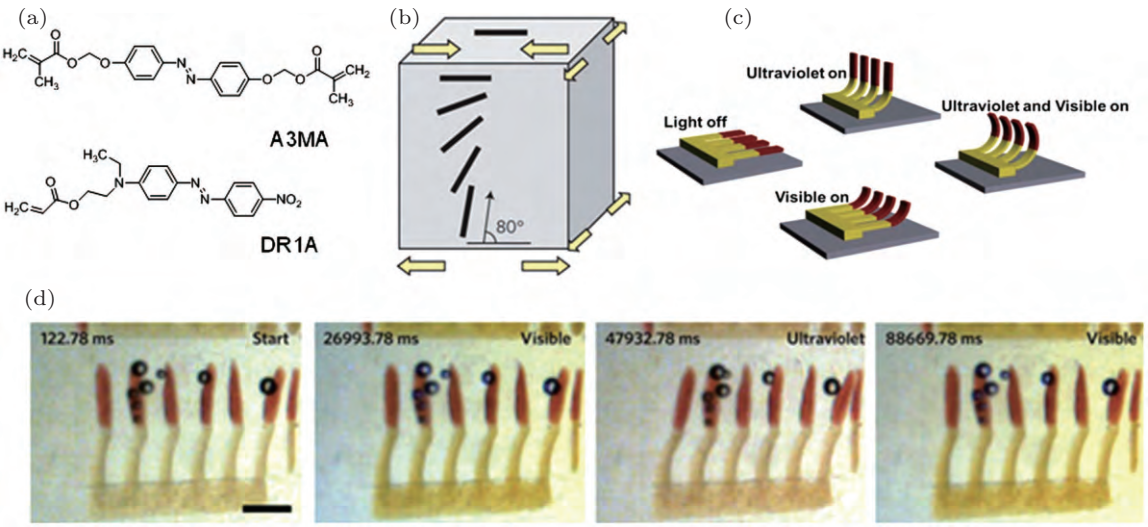

Fig. 16. (color online) (a) Chemical structures of yellow dye A3MA and red dye DR1A. (b) Schematic illustration of the molecular alignment of the splayed structure through the thickness of the film. (c) Schematic representation of the photo-driven asymmetric motion produced by artificial cilia. (d) Front view of multicolour cilia motion in water irradiated with visible (4 mW/cm^2) and UV (9 mW/cm^2) light. Scale bar: 0.5 mm. Reprinted with permission from Ref. [69].

Recently, considerable interests have been focused on photoresponsive CLCP films with micro- or nano-structures due to their potential applications in microfluid and optics, etc. Our group successfully prepared micro-arrayed CLCP films by polydimethylsiloxane (PDMS) soft-template-based secondary replication, which showed an ideal quick (< 1 min) and reversible switch of superhydrophobic adhesion by alternating irradiation of UV–visible light (Fig. 17).[70] Unlike CA switchable surfaces systems, our work put emphasis on the switching of sliding angle (SA) on the same surface, while the static CAs before and after switching were all in the superhydrophobic range. Therefore, the "rolling" and "pinning" of water droplets was achieved, giving rising to promising applications in microfuids. It is the first time that the photoresponsive CLCP materials were used to prepare superhydrophobic adhesion switchable surfaces, which is of great importance for no-loss microdroplet transfer.

The size of the arrays in CLCP films with different surface topographies (pillars and cones) was further diminished to nanoscale through colloidal lithography technique by utilizing different types of etching masks (Fig. 18).[71] Interestingly, these two types of films with the same chemical structure showed completely different wetting behaviors of water adhesion, which mimicked rose petal and lotus leaf, respectively. Both types of the submicro-arrayed films demonstrated superhyrophobicity, while the submicropillar arrayed film exhibited a very high sliding angle (SA) greater than 90° which could pin the water droplet like rose petal and the submicro-

cone arrayed film showed a small SA of only $3.1^\circ \pm 2.0^\circ$. Compared to the replica molding technique and inkjet printing technology used to fabricate microstructured CLCPs, the colloidal lithography technique is time-saving and can be modulated throughout etching procedure, which finely regulate the structural parameters such as shapes and dimensions. Our work provides a new way to fabricate the CLCPs in the size of nanoscale.

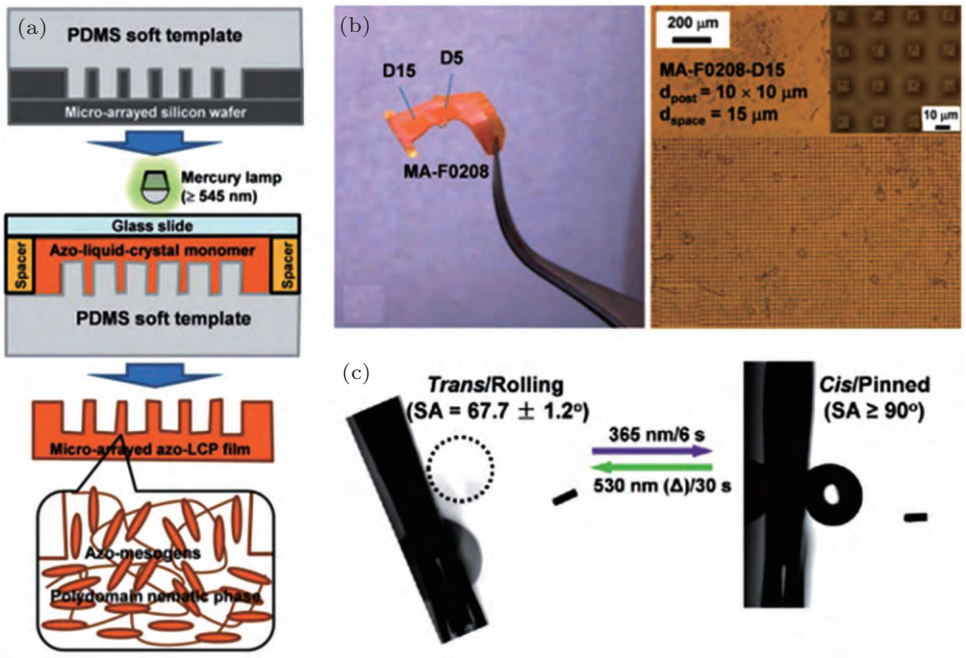

Fig. 17. (color online) (a) Schematic representation of the fabrication process. (b) Optical photograph and microscopic image of the microarrayed CLCP film. (c) Light-driven fast and reversible switching of a 2 mL water droplet between rolling and pinning states on the superhydrophobic CLCP film. Reprinted with permission from Ref. [70].

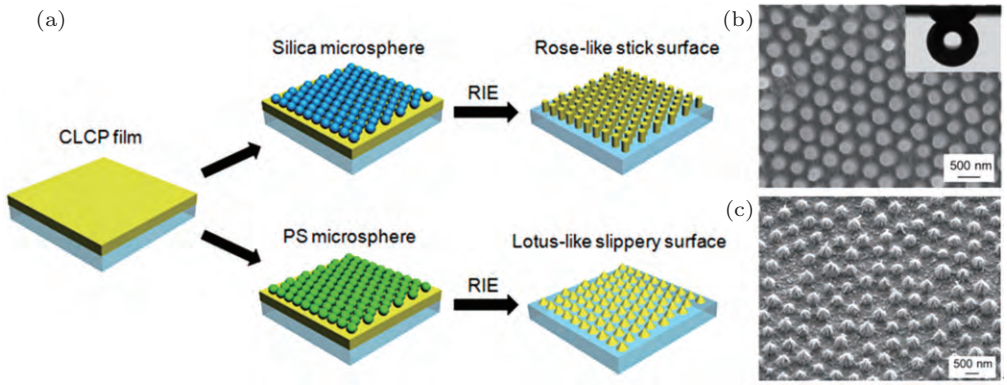

Fig. 18. (color online) (a) Schematic procedure of the fabrication of microarrayed CLCP films. (b) SEM image of submicropillar arrayed CLCP film. Inset: The shape of a water droplet on the CLCP film when it is turned upside down, indicating its high water adhesion. (c) SEM image of the surface of submicrocone arrayed CLCP film. Reprinted with permission from Ref. [71].

Except for the reversible switch of water adhesion mentioned above, on-off switch behavior on the reflection spectra of the microarrayed two-dimensional (2D) CLCP photonic crystal was also observed by alternate irradiation with UV–visible light.[72] It is the first time to fabricate the microarray with a period of about 1 μm from the CLCPs and tune the reflection spectra of the CLCP microarray by light. In comparison to 2D photonic crystals, inverse opal materials (3D photonic crystals) have exhibited superior photonic crystal properties, such as especially high reflection intensity and tunable color changes. Therefore, our group further prepared CLCP inverse opal films which demonstrated a switchable behavior on the reflection spectra resulting from the order change of the holes by alternate irradiation of UV–visible light or variation of temperature (Fig. 19).[73] The reflectivity changed to a greater extent compared to the 2D CLCP photonic crystals.

Most recently, Wiersma *et al.* used a direct laser writing system to pattern the complex 3D CLCP structures with sub-micrometer resolution.[74,75] Microrobots were therefore fabricated with the CLCPs acting as the walker's main body.[75] The photo induced maximum stress was 260 ± 2 kPa, which was comparable to natural muscles (10–200 kPa). The

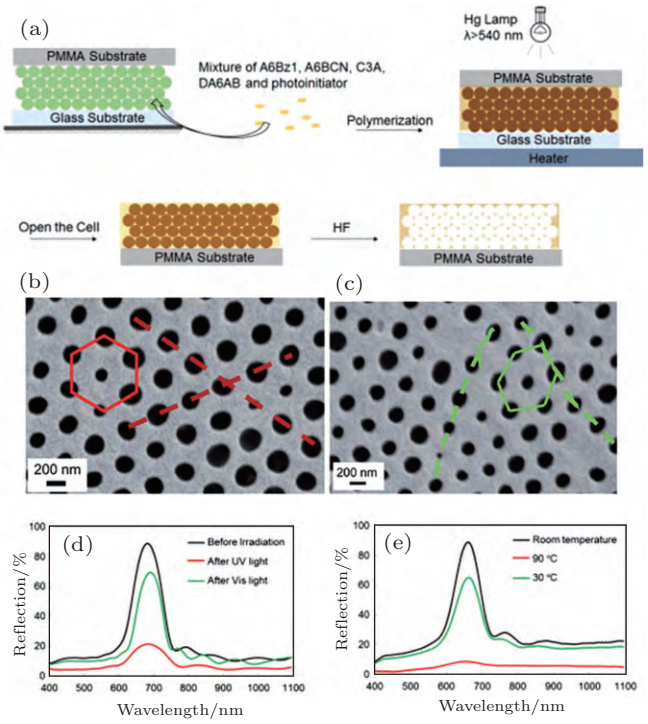

Fig. 19. (color online) (a) The preparation process of the CLCP inverse opal film. (b), (c) SEM images of the CLCP inverse opal film (b) before and (c) after the irradiation of UV light. (d) Reflection spectra of the CLCP inverse opal film under UV and subsequent visible light irradiation. (e) Reflection spectra of the CLCP inverse opal film through heating and cooling process. Reprinted with permission from Ref. [73].

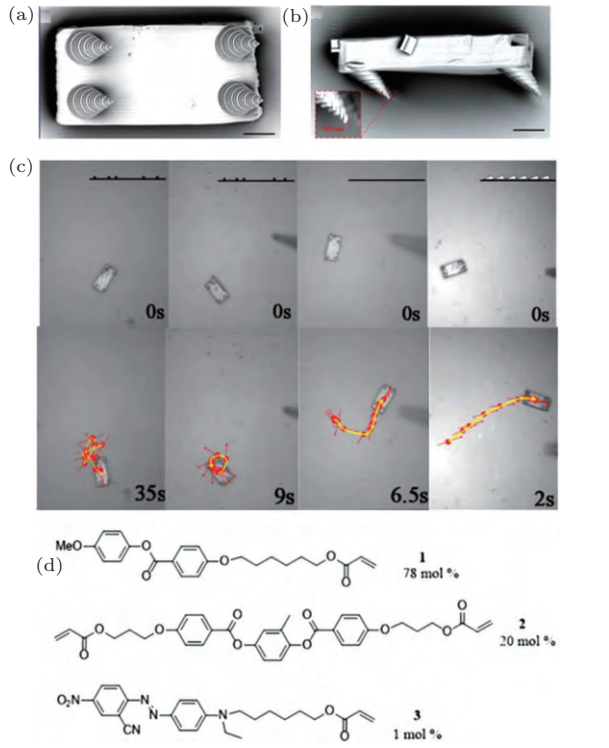

Fig. 20. (color online) SEM images of a microwalker from (a) bottom and (b) side view. Scale bar: 10 μm. (c) Top row shows the initial state of microwalkers on different surfaces. Bottom row shows the microwalker randomly walking, rotating, walking with self-reorientation, and walking along certain direction. (d) Molecules used in the experiment on different surfaces. Insets of the top row show the schematics of the surface. Reprinted with permission from Ref. [75].

walker's leg had a conical shape which was designed to decrease the surface contact area, while 45° tilt of the leg created the adhesion asymmetry necessary for walking (Figs. 20(a) and 20(b)). The microscopic walker finished random walking, rotating, directional walking, and jumping when placed on surfaces with different treating methods (Fig. 12(c)).

5. Conclusion and perspectives

In conclusion, we have reviewed thermo- or photo-controllable CLCP actuators achieved via order changes of mesogens within a polymer network. The particularly large and reversible dimensional change and the appropriate stress that thermoresponsive CLCPs generate by phase transition provide great advantages to mimic artificial muscles. As the earliest developed CLCPs, numerous studies have been done on the thermoresponsive CLCPs. Various types of thermo-driven CLCP actuators including microvalves, micropumps for microfluids, and tunable aperture mimicking the human iris have been developed. To implement contactless and precise control, soft CLCP actuators driven by absorptive heating with either optical or magnetic stimuli have also been fabricated. Therefore, the development of thermoresponsive CLCPs and the actuators based on them has become more and more complete.

The incorporation of photochromic moieties makes it possible for the CLCPs to be photoresponsive and the resultant actuators are able to be photo-driven. Due to their photo-controllable properties without any aid of other motors, gears, and wires, it is very convenient and attractive to reduce the size of the photo-driven CLCP actuators for their potential application in micro and even nano scales. So far, based on the replica molding and inkjet printing technique, microarrayed CLCP films and the cilia-like microactuator have been successfully developed, which are of great use in the manipulation and transport of microdroplets. In addition, the size of the photo-driven actuators has been successfully diminished to the nanoscale by the colloidal lithography technique. Light is an especially fascinating stimulus, which can be precisely adjusted from the perspective of polarization direction, wavelength, and intensity, allowing noncontact control. These factors make it advantageous to use photo-driven actuators in micro-opto-mechanical systems (MOMS). Microarrayed and the inverse opal CLCP films that exhibited repeatable switching behavior of the reflection spectra were successfully fabricated, which offers the application of photo-driven CLCP actuators in optics.

Further efforts to develop thermo- or photo-controllable CLCP actuators are still needed to make them of value in real life applications. For instance, the challenges that remain for researchers to solve include improvement of the energy conversion efficiency, fatigue resistance and strength, and the continuous production of CLCPs. In addition, there is an urgent need to integrate the CLCPs into functional and sophisticated devices with other materials because of the difficulty of the stimuli-responsive CLCPs to serve as whole smart devices in real applications.

References

[1] Shankar R, Ghosh T K and Spontak R J 2007 *Soft Matter* **3** 1116
[2] Yao S and Zhu Y 2015 *Adv. Mater.* **27** 1480
[3] Wang Y, Chen H, Liu J, Zhu Z, Chang L, Li D and Jia S 2015 *J. Polym. Eng.* **35** 611
[4] Chollet F 2016 *Micromachines* **7** 18
[5] Tomatsu I, Peng K and Kros A 2011 *Adv. Drug Delivery Rev.* **63** 1257
[6] Ponmozhi J, Frias C, Marques T and Frazao O 2012 *Measurement* **45** 1675
[7] Langbein S and Czechowicz A 2015 *Shape Memory Alloy Valves* (New York: Springer International Publishing) pp. 41–72
[8] Friend J and Yeo L 2015 *Encyclopedia of Microfluidics and Nanofluidics* (New York: Springer) pp. 2743–2754
[9] Finkelmann H 1987 *Angew. Chem. Int. Ed.* **26** 816
[10] Zentel R 1989 *Angew. Chem. Int. Ed.* **28** 1407
[11] Kelly S M 1995 *J. Mater. Chem.* **5** 2047
[12] Ohm C, Brehmer M and Zentel R 2010 *Adv. Mater.* **22** 3366
[13] Ikeda T, Mamiya J and Yu Y L 2007 *Angew. Chem. Int. Ed.* **46** 506
[14] Bar-Cohen Y and Zhang Q M 2008 *Mrs Bull.* **33** 173
[15] de Gennes P 1975 *CR Acad. Sci. B* **281** 101
[16] de Gennes P G, Hebert M and Kant R 1997 *Macromol. Symp.* **113** 39
[17] Kupfer J and Finkelmann H 1991 *Makromol. Chem-Rapid.* **12** 717
[18] Wermter H and Finkelmann H 2001 *e-Polymers* 13
[19] Li M H, Keller P, Yang J Y and Albouy P A 2004 *Adv. Mater.* **16** 1922
[20] Wei R B, Zhang H X, He Y N, Wang X G and Keller P 2014 *Liq. Cryst.* **41** 1821
[21] Buguin A, Li M H, Silberzan P, Ladoux B and Keller P 2006 *J. Am. Chem. Soc.* **128** 1088
[22] Mol G N, Harris K D, Bastiaansen C W M and Broer D J 2005 *Adv. Funct. Mater.* **15** 1155
[23] Sawa Y, Ye F F, Urayama K, Takigawa T, Gimenez-Pinto V, Selinger R L B and Selinger J V 2011 *Proc. Nat. Acad. Sci. USA* **108** 6364
[24] Ware T H, McConney M E, Wie J J, Tondiglia V P and White T J 2015 *Science* **347** 982
[25] Ho C M and Tai Y C 1998 *Annu. Rev. Fluid. Mech.* **30** 579
[26] Ohm C, Serra C and Zentel R 2009 *Adv. Mater.* **21** 4859
[27] Ohm C, Fleischmann E K, Kraus I, Serra C and Zentel R 2010 *Adv. Funct. Mater.* **20** 4314
[28] Fleischmann E K, Liang H L, Kapernaum N, Giesselmann F, Lagerwall J and Zentel R 2012 *Nat. Commun.* **3** 1178
[29] Ohm C, Morys M, Forst F R, Braun L, Eremin A, Serra C, Stannarius R and Zentel R 2011 *Soft Matter* **7** 3730
[30] Yang H, Buguin A, Taulemesse J M, Kaneko K, Mery S, Bergeret A and Keller P 2009 *J. Am. Chem. Soc.* **131** 15000
[31] Wu Z L, Buguin A, Yang H, Taulemesse J M, Le Moigne N, Bergeret A, Wang X G and Keller P 2013 *Adv. Funct. Mater.* **23** 3070
[32] Ohm C, Haberkorn N, Theato P and Zentel R 2011 *Small* **7** 194
[33] Sanchez-Ferrer A, Fischl T, Stubenrauch M, Wurmus H, Hoffmann M and Finkelmann H 2009 *Macromol. Chem. Phys.* **210** 1671
[34] Sanchez-Ferrer A, Fischl T, Stubenrauch M, Albrecht A, Wurmus H, Hoffmann M and Finkelmann H 2011 *Adv. Mater.* **23** 4526
[35] Schuhladen S, Preller F, Rix R, Petsch S, Zentel R and Zappe H 2014 *Adv. Mater.* **26** 7247
[36] Chambers M, Finkelmann H, Remskar M, Sanchez-Ferrer A, Zalar B and Zumer S 2009 *J. Mater. Chem.* **19** 1524
[37] White T J and Broer D J 2015 *Nat. Mater.* **14** 1087
[38] Chambers M, Zalar B, Remskar M, Zumer S and Finkelmann H 2006 *Appl. Phys. Lett.* **89** 243116
[39] Kaiser A, Winkler M, Krause S, Finkelmann H and Schmidt A M 2009 *J. Mater. Chem.* **19** 538
[40] Riou O, Lonetti B, Davidson P, Tan R P, Cormary B, Mingotaud A F, Di Cola E, Respaud M, Chaudret B, Soulantica K and Mauzac M 2014 *J. Phys. Chem. B* **118** 3218
[41] Haberl J M, Sanchez-Ferrer A, Mihut A M, Dietsch H, Hirt A M and Mezzenga R 2013 *Adv. Mater.* **25** 1787
[42] Yang L Q, Setyowati K, Li A, Gong S Q and Chen J 2008 *Adv. Mater.* **20** 2271
[43] Ji Y, Huang Y Y, Rungsawang R and Terentjev E M 2010 *Adv. Mater.* **22** 3436
[44] Camargo C J, Campanella H, Marshall J E, Torras N, Zinoviev K, Terentjev E M and Esteve J 2011 *Macromol. Rapid Commun.* **32** 1953
[45] Camargo C J, Torras N, Campanella H, Marshall J E, Zinoviev K, Campo E M, Terentjev E M and Esteve J 2011 *Proc. SPIE* **8107** 810709
[46] Marshall J E, Ji Y, Torras N, Zinoviev K and Terentjev E M 2012 *Soft Matter* **8** 1570
[47] Liu X Y, Wei R B, Hoang P T, Wang X G, Liu T and Keller P 2015 *Adv. Funct. Mater.* **25** 3022
[48] de Haan L T, Sanchez-Somolinos C, Bastiaansen C M W, Schenning A P H J and Broer D J 2012 *Angew. Chem. Int. Ed.* **51** 12469
[49] Kohlmeyer R R and Chen J 2013 *Angew. Chem. Int. Ed.* **52** 9234
[50] Li C S, Liu Y, Huang X Z and Jiang H R 2012 *Adv. Funct. Mater.* **22** 5166
[51] Wei J and Yu Y L 2012 *Soft Matter* **8** 8050
[52] Yu Y L and Ikeda T 2006 *Angew. Chem. Int. Ed.* **45** 5416
[53] Wang W, Wang X Z, Cheng F T, Yu Y L and Zhu Y T 2011 *Prog. Chem.* **23** 1165 (in Chinese)
[54] Zhang B Z, Cui H and She W L 2009 *Chin. Phy. B* **18** 209
[55] Dong Y, Shen D and Zheng Z G 2012 *Chin. J. Liq. Cryst. Disp.* **27** 14
[56] Zhou L, Zhang D, Zheng Z G, Shen D and Bao X F 2013 *Chin. J. Liq. Cryst. Disp.* **28** 7 (in Chinese)
[57] Ube T and Ikeda T 2014 *Angew. Chem. Int. Ed.* **53** 10290
[58] Finkelmann H, Nishikawa E, Pereira G G and Warner M 2001 *Phys. Rev. Lett.* **87** 015501
[59] Ikeda T, Nakano M, Yu Y L, Tsutsumi O and Kanazawa A 2003 *Adv. Mater.* **15** 201
[60] Yu Y L, Nakano M and Ikeda T 2003 *Nature* **425** 145
[61] Yamada M, Kondo M, Mamiya J I, Yu Y L, Kinoshita M, Barrett C J and Ikeda T 2008 *Angew. Chem. Int. Ed.* **47** 4986
[62] Yamada M, Kondo M, Miyasato R, Naka Y, Mamiya J, Kinoshita M, Shishido A, Yu Y L, Barrett C J and Ikeda T 2009 *J. Mater. Chem.* **19** 60
[63] Yin R Y, Xu W X, Kondo M, Yen C C, Mamiya J, Ikeda T and Yu Y L 2009 *J. Mater. Chem.* **19** 3141
[64] Cheng F T, Zhang Y Y, Yin R Y and Yu Y L 2010 *J. Mater. Chem.* **20** 4888
[65] Cheng F T, Yin R Y, Zhang Y Y, Yen C C and Yu Y L 2010 *Soft Matter* **6** 3447
[66] Chen M L, Xing X, Liu Z, Zhu Y T, Liu H, Yu Y L and Cheng F T 2010 *Appl. Phys. A* **100** 39
[67] Chen M L, Huang H T, Zhu Y T, Liu Z, Xing X, Cheng F T and Yu Y L 2011 *Appl. Phys. A* **102** 667
[68] Iamsaard S, Asshoff S J, Matt B, Kudernac T, Cornelissen J J L M, Fletcher S P and Katsonis N 2014 *Nat. Chem.* **6** 229
[69] van Oosten C L, Bastiaansen C W M and Broer D J 2009 *Nat. Mater.* **8** 677
[70] Li C, Cheng F T, Lv J A, Zhao Y, Liu M J, Jiang L and Yu Y L 2012 *Soft Matter* **8** 3730
[71] Zhan Y Y, Zhao J Q, Liu W D, Yang B, Wei J and Yu Y L 2015 *Acs Appl. Mater. Interfaces* **7** 25522
[72] Yan Z, Ji X M, Wu W, Wei J and Yu Y L 2012 *Macromol. Rapid. Commun.* **33** 1362
[73] Zhao J Q, Liu Y Y and Yu Y L 2014 *J. Mater. Chem. C* **2** 10262
[74] Zeng H, Martella D, Wasylczyk P, Cerretti G, Lavocat J C G, Ho C H, Parmeggiani C and Wiersma D S 2014 *Adv. Mater.* **26** 2319
[75] Zeng H, Wasylczyk P, Parmeggiani C, Martella D, Burresi M and Wiersma D S 2015 *Adv. Mater.* **27** 3883